ACS OMEGA

Open Access

http://pubs.acs.org/journal/acsodf

Article

A Soy Protein-Based Film Based on Chemical Treatment and Microcrystalline Cellulose Reinforcement Obtained from Corn Husk Byproducts

Binghan Zhang,* Baicheng Guo, Shihan Wang, Can Liu, Lu Cheng, and Jinguo Wang*

Cite This: *ACS Omega* 2024, 9, 15845−15853

Read Online

ACCESS | Metrics & More | Article Recommendations

ABSTRACT: Developing an environmentally friendly soy protein-based film that offers excellent performance has garnered considerable interest while also posing a significant challenge. Herein, we propose the strategy of covalent and noncovalent cross-linking to improve the mechanical properties of the films. First, chemical denaturation was carried out under the combined action of sodium sulfite, sodium dodecyl sulfate, sodium hydroxide, and urea to reshape the structure of the protein to improve the solubility of protein and release active groups. Then, microcrystalline cellulose (MCC) derived from low-cost agro-industrial byproducts (corn husk) was employed to balance the covalent cross-linking reaction between proteins and the noncovalent reaction between MCC and protein. The results indicate that the structure and properties of the soy protein-based films were modified and improved through chemical treatment in conjunction with biomass enhancement. It is concluded that the addition of 1% MCC improves the tensile strength, elastic modulus, water solubility, and water vapor permeability of "MCC-1%" by 64.7, 75.9, 22.7, and 12.9%, respectively. Additionally, the resulting film of "MCC-1%" exhibits better resistance to thermal degradation and improved thermo-stability. However, the elongation at break decreased by increasing the addition of MCC. Thus, this work may provide a simple and affordable approach to preparing a high-performing soy protein-based film.

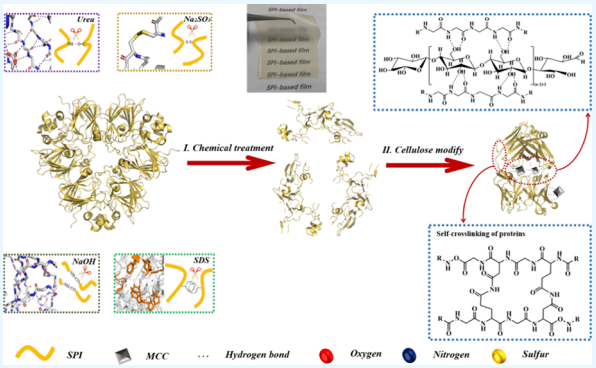

1. INTRODUCTION

Nonbiodegradable polymer films can bring a series of problems such as water pollution and global warming. It is essential to develop packaging materials that are safe and biodegradable and have good preservation performance.[1] Several researchers have conducted theoretical studies on different biological macromolecules as film-forming substrates, including starch, chitin, cellulose, protein, and others, applying the films based on them in food packaging and preservation, electrode materials, biomedicine, and other fields.[2−9] Among these biomass materials, soy protein has garnered significant attention due to its good film-forming properties, processability, biocompatibility, abundance, environmental friendliness, and renewability. However, the limited properties of soy protein-based films, such as high water vapor permeability, brittleness, and poor mechanical strength, have hindered their widespread application.[10]

Soy protein, which is the main byproduct obtained from the extraction and processing of soybean oil, possesses a compact and highly organized collapsed globular structure. Its main functional groups, including amino, hydroxyl, and carboxylic groups, are buried within globular particles. Additionally, weak intermolecular interactions (such as hydrogen bonds, electrostatic bonds, van der Waals forces, disulfide bonds, and hydrophobic interactions) are the primary force to build the complex quaternary structure of proteins. However, these interactions are susceptible to degradation, particularly when exposed to water erosion, especially hot or boiling water.[11] Therefore, many efforts have focused on improving the film properties by modifying the soy protein, mainly including protein molecular modification, cross-linking modification, enzyme treatment, organic−inorganic hybrid development, nanomaterial incorporation, etc.[12−16]

Acid, alkali, salt, urea, sodium dodecyl sulfate, and sodium sulfite are the main reagents used to unfold the protein structure and expose more reactive groups, or grafting modification is then employed to further enhance the

Received: October 10, 2023
Revised: February 28, 2024
Accepted: March 18, 2024
Published: March 27, 2024

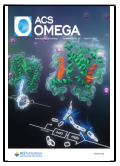

https://doi.org/10.1021/acsomega.3c07907
ACS Omega 2024, 9, 15845−15853

properties of soy protein-based films.[17−23] This enzymatic technique has significant potential for expanding the utilization of active groups in a soy protein isolate (SPI) safely. For instance, transglutaminase can catalyze the formation of heterotypic peptide bonds between the amino groups of lysine residues and the carboxamide groups of glutamine residues in different proteins, resulting in tighter molecular structures.[6] Recently, many researchers constructed organic−inorganic hybrid structures in soy protein-based film systems by introducing inorganic nanoparticles. This approach provides an effective means of producing films with a high bond strength and toughness.[24] However, soy protein-based films still have certain limitations that hinder their widespread and diverse applications in the packaging material industry, such as poor mechanical properties and high water vapor permeability.

As an eco-friendly and sustainable alternative for enhancing composites, natural reinforcing biomaterials have gained popularity. Natural cellulose, in particular, offers several advantages, such as a high length-to-diameter ratio, biodegradability, low density, and excellent mechanical performance, making it an ideal choice for composite enhancement. Nanocelluloses are suitable for a variety of applications, including the production of composites, paperboard, coating additives, cosmetics, pharmaceuticals, electronic devices, and others. For example, the coloring efficiency could be improved by nanocellulose in the production of colored paper, thus decreasing the environmental impact of the manufacturing process.[25] Certainly, different sources of cellulose have been used to modify the properties of soy protein-based films, particularly mechanical strength and water vapor permeability, including sugar cane bagasse and other lignocellulosic materials or other synthetic celluloses.[26,27] Among them, corn husk, the packaged part of the corn cob, is one of the more attractive raw materials, which has a high concentration of cellulose (38.2%) and hemicellulose (44.5%) and just a little amount of lignin (6.6%) and ash (2.8%).[28] Compared to wood fiber, corn husk has excellent strength, acceptable pliability, moderate durability, high elongation, etc. There were more than 1129 million tons of corn produced in the world in 2021, and corn husks represent about 7% of corn production. However, the present situation is that these resources are discarded or burned and have not yet been fully utilized, which must be processed properly, or there will be significant environmental strain. Consequently, it is crucial to turn corn husks into useful products.[29]

In this study, urea, SDS, Na_2SO_3, and NaOH were used as common denaturants to enhance the performance of soy protein-based films. These denaturants were employed to moderately disrupt the higher structure of the protein, thereby releasing active groups. A previous study has demonstrated that urea, rich in oxygen and nitrogen, is capable of effectively unfolding hydrogen bonds and hydrophobic interactions within the protein structure. As a result, it facilitated the unfolding of the quaternary and tertiary structure of soy protein molecules.[30] SDS, functioning as an anionic surfactant, primarily disrupted the hydrophobic bonds of soy protein molecules, leading to the unfolding of their quaternary structure.[31] Na_2SO_3 as a reducing agent could effectively reduce the disulfide bond (−S−S−) inside and outside the polypeptide chain of soy protein molecules to sulfhydryl (−SH), thus unfolding the secondary and tertiary structure of soy protein molecules.[32] Then, low-dose NaOH was added to hydrolyze the primary structures of protein partially.[33] On this basis, natural cellulose derived from corn husk was selected to enhance the properties of the films, and its effects in the presence of urea, SDS, Na_2SO_3, and NaOH were investigated.

2. MATERIALS AND METHODS

2.1. Materials. SPI with a protein content of over 94% and a particle size smaller than 0.096 mm was acquired from Harbin High-Tech Soybean Food Co., Ltd. in Harbin, China. MCC was prepared in our lab. H_2SO_4 was purchased from Shanghai McLean Biochemical Technology Co., Ltd., Shanghai, China. Reagent-grade urea (with a content of 99%), SDS (with a content of 99.7%), Na_2SO_3 (with a content of 97%), NaOH (with a content of 99.5%), and glycerol (with a content of 99%) were purchased from Tianjin Kermel Chemical Reagent Co., Ltd., Tianjin, China. H_2O_2 was purchased from Linyi Yujiang Trading Co., Ltd., Linyi, China.

2.2. Extraction of Cellulose and Preparation of MCC. Corn husks (100 g) were weighed, washed, and dried (<5%) in an oven at 60 °C until a low-moisture product was obtained and then cut into small pieces with scissors followed by milling using a pulverizer (FW100, China). The resulting powder was treated in a NaOH solution (1 mol·L^{-1}) for 2 h at 60 °C to solubilize the lignin and hemicellulose in the corn husks. The suspension was centrifuged (2000 rpm, 5 min) and washed with portions of distilled water to reach pH 7. The sample was then subjected to a bleaching process using a H_2O_2 solution (30%) for 2 h at 60 °C. This step was followed by repeating the centrifugation and washing procedures. Cellulose powder extracted according to the above method was dispersed in distilled water and stirred for 4 h at 60 °C, and then, H_2SO_4 (60%) was dropped in the mixed liquid. The mixture was cooled in an ice water bath and diluted to 10 times its original volume to stop the reaction. Then, the mixture was centrifuged, and the resulting solid was placed in a dialysis bag to separate H_2SO_4 from the mixed liquid until the dialysate became neutral. MCC with a smaller particle size can be obtained by centrifuging the mixture to retain a white solid. Finally, the white solid was freeze-dried and stored.

2.3. Preparation of the Film-Forming Solution and Soy Protein-Based Film. The film-forming solution was prepared by dissolving SPI (6 g) in distilled water (91 mL) with glycerin (3 g) while stirring continuously for 2 h at 75 °C and labeled as S1. The film-forming solution S2 was developed by dissolving SPI (6 g) in distilled water (91 mL) in the presence of urea (0.3 g), SDS (0.06 g), Na_2SO_3 (0.06 g), NaOH (0.06 g), and glycerin (3 g) under continuous stirring for 2 h at 75 °C. Various weights of MCC (0, 1, 2, 3, 4, and 5% on an SPI basis) were added to the film-forming solutions, which were prepared in the same way as S2, and the mixture was ultrasonically dissolved in distilled water (20 mL) for 0.5 h. Then, the pH of the resulting solution was adjusted to 8.5 with NaOH (1.0 mol·L^{-1}). Finally, the film-forming solutions with the same quantity (50 mL) were poured onto a 15 cm × 15 cm polytetrafluoroethylene mold, dried at 55 °C for 12 h and conditioned at 43 ± 2% relative humidity (RH) for 24 h before testing, and labeled as "MCC-0%", "MCC-1%", "MCC-2%", "MCC-3%", "MCC-4%", and "MCC-5%", respectively.

2.4. Characterization. *2.4.1. Particle Size Test.* The particle size test of MCC was implemented using a Mastersizer 3000 laser particle sizer produced by Malvern Panalytical Company affiliated with Spectris Instrument System Co. (Shanghai, China), Ltd. MCC powder (2 g) was weighed and dispersed in 800 mL of distilled water with ultrasonic

https://doi.org/10.1021/acsomega.3c07907
ACS Omega 2024, 9, 15845−15853

treatment for 30 min and then tested by wet dispersion at room temperature.

2.4.2. Gel Permeation Chromatography (GPC) Test of Film-Forming Solution. A reaction kettle, equipped with a mechanical stirrer and refluxing equipment, was charged with film-forming solution (5 g) and urea solution (100 g, 8 mol·L^{-1}). The mixture was maintained at 50 ± 2 °C for 2.5 h with continuous stirring to ensure homogeneous mixing. During this process, some of the urea might convert to ammonia due to the presence of urease in the film-forming solution, without the need for de-enzyme or thermal treatment. However, the concentration of urea (8 mol·L^{-1}) was sufficient for complete dissolution of the sample. After that, the resulting product was cooled to room temperature and then filtered by using a glass fiber filter. The filtered solution was then diluted to 0.1 wt % with deionized distilled water before the determination of the molecular weight (MW) using an Agilent 1100 GPC according to the method of Li et al.[34]

2.4.3. Acetaldehyde Value of Film-Forming Solution. Film-forming solution (25 mL, its solid fraction was measured and recorded as m_1), 50 mL of distilled water, and acetaldehyde solution (5 mL, 40%) were added into a 100 mL flask with a mechanical stirrer, a thermostat, and a reflux condenser. Then, 20 wt% NaOH solution was used to adjust the pH of the mixture to 8.5−8.7. The mixture was then stirred mechanically for 2 h at 50 °C and allowed to cool to room temperature. After that, the mixture was diluted to 1000 mL in a volumetric flask. The acetaldehyde value of the two film-forming solutions was tested according to the method in the reference.[34] Three blank tests were carried out under the same situations but without the film-forming solution to calculate the total free acetaldehyde concentration (F_1, mmol·L^{-1}) before the reaction. The acetaldehyde value (mg·g^{-1}) of the sample was defined as the equivalent mass of acetaldehyde (mg) that can react with 1g of the solid fraction of film-forming solution and was calculated using

$$(F_1 - F_2) \times 44m_1$$

In a weakly alkaline environment, acetaldehyde can occur in a nucleophilic addition reaction with free amino in proteins and then remove a molecule of water to form a Schiff base, so the acetaldehyde value of film-forming solution represented the extent to which active groups in the protein structure were exposed.[35]

2.4.4. Fourier Transform Infrared Spectroscopy (FTIR). FTIR spectra of different samples were carried out on a Nicolet iS50 spectrometer (USA). Since the sample thickness and the potassium bromide/protein ratio may differ from one another, the internal standard approach was used to calculate the precise group concentrations of diverse samples. The C−H vibration's peak, measured at approximately 2930 cm^{-1}, was used as an internal standard.

2.4.5. X-ray Diffraction Spectroscopy (XRD) Analysis. The changes in the crystalline structure of the film-forming solution and film-forming solution of chemical treatment were investigated by using a D/MAX-2200 diffractometer (Rigaku, Tokyo, Japan) with a Cu Kα source. Diffraction data were collected from 5 to 50° with a step interval of 0.02° at 40 kV and 30 mA.

2.4.6. Film Thickness Test. Each film sample was measured six times to determine its thickness using a digital micrometer (Wuxi Xigong Measuring Tools Co., Ltd., China), which has a 0.002 mm precision. The study of three duplicates produced the average film thickness results.

2.4.7. Mechanical Strength (MS) Test. Ten specimens with a bond area of 1 mm × 15 mm were cut out of each manufactured film to determine the tensile strength (TS), elastic modulus (EM), and elongation at break (EB). The tests were carried out using tensile testing with a crosshead speed of 5 mm·min^{-1} at room temperature following the standard ASTM D882/12.

2.4.8. Scanning Electron Microscopy (SEM). The surface of the gold-coated films was analyzed by SEM (Gemini SEM 3000, Carl Zeiss, Oberkochen, Germany), operating at 5 kV.

2.4.9. Water Solubility (WS). Beakers were weighted (m_1, accurate to 0.0001 g), and film samples with various contents of MCC of 150 × 15 mm were added into different beakers and then weighted (m_2, accurate to 0.0001 g). After that, 100 mL of distilled water was added to the beakers to immerse the film. After 12 h, the water was poured off, and the beakers were placed in a vacuum oven to dry at 120 °C to a constant weight (m_3, accurate to 0.0001 g). Photographs were taken and recorded every hour during this period. Finally, the WS of the film was calculated according to the calculation formula, which is as follows:

$$W_{WS} = \frac{m_2 - m_3}{m_2 - m_1} \times 100\%$$

2.4.10. Water Vapor Permeability (WVP). The test of WVP was conducted according to the method of a reference paper.[36] Specimens with a bond area of 40 × 25 mm were cut to seal over a weighing bottle using liquid paraffin, and the weighing bottle with anhydrous calcium chloride (2.5 g) was dried in an oven at 120 °C for 2 h. After that, the finished weighing bottle was weighed (m_1) and then put into a desiccator with saturated sodium chloride solution while maintaining constant humidity (90%) and temperature (25 °C). The weight change of the weighing bottle was recorded after 24 h and denoted as m_2. Finally, the WVP of the film was calculated according to the calculation formula, which is as follows:

$$W_{WVP} = \frac{(m_2 - m_1)d}{At\Delta p}$$

where WVP (g·mm·h^{-1}·m^{-2}·kPa^{-1}) is the water vapor permeability; $m_2 - m_1$ (g) is the mass of water vapor absorbed by anhydrous calcium chloride in this process; d (mm) is the thickness of the film; A (m^2) is the effective area of the film; t (h) is the test time; Δp (kPa) is the water vapor pressure difference between the two sides of the film.

2.4.11. Light Transmittance. The light transmittance of the film was determined using a 722G spectrophotometer (Shanghai Precision Scientific Instrument Corporation, China) at a wavelength of 600 nm. The film was cut into a rectangular shape measuring 10 × 30 mm and placed on one side of a colorimetric cell.

2.4.12. Thermogravimetric Analysis (TGA). The cured film samples were individually analyzed by using a Netzsch 209 F3 TGA instrument. The analysis was conducted from room temperature up to 750 °C, with a heating rate of 10 °C ·min^{-1}, while maintaining a nitrogen purge flow of 25 mL ·min^{-1}.

2.5. Statistical Analysis. The data were analyzed using Excel, and the results were presented as means ± standard deviation. To determine significant differences among the mean values, a one-way analysis of variance (ANOVA) was

https://doi.org/10.1021/acsomega.3c07907
ACS Omega 2024, 9, 15845−15853

performed. A significance level of $P < 0.05$ was used to determine statistical significance.

3. RESULTS AND DISCUSSION

3.1. Characterization and Analysis of Film-Forming Solution. Soybean protein has poor solubility in room-temperature water due to its high molecular weight and compact globular structure, which is built by weak intermolecular interactions, including hydrogen bonds, electrostatic bonds, and hydrophobic interactions.[37] It will gradually dissolve in water at elevated temperatures because of the destruction of weak intermolecular interactions. However, precipitation will occur with the extension of standing time (as shown in Figure 1), which is because the unfolding of the

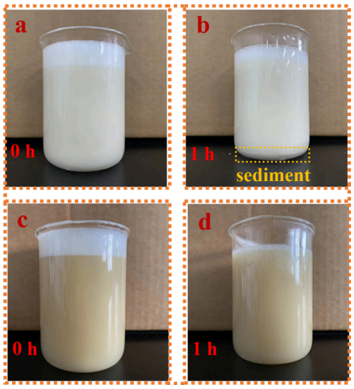

Figure 1. Digital photographs of the film-forming solution (a,b) without denaturing agents and (c,d) with denaturing agents.

protein structure and the extension of the molecular chain can expose more active groups in the process of dissolving and dispersing. As a result, the dissolved soybean protein molecular segments are rearranged and aggregated into a higher-order structure to precipitate out. This phenomenon has a profound impact on the structure and performance of soy protein-based films.

To solve this problem, the combined modifications composed of urea, Na_2SO_3, SDS, and a moderate concentration of NaOH were used to prepare a soybean protein liquefied product as the matrix of the films, achieving good dispersion of proteins in aqueous solutions. As shown in Figure 2a, the molecular weight of the protein in S2 was approximately 68,600, which was much lower than in the natural soy protein that ranged from 150,000 to 360,000 and also lower than in S1 with about 91,200.[38] This was due to the unfolding of the supramolecular spherical structure and moderate degradation of molecular chains. Meanwhile, Figure 2b shows that the absorption peak intensities at 3274 cm^{-1} (N−H and O−H stretching) were marked increased, and the absorption peak intensities at 1638 (amide I, C═O stretching), 1530 (amide II, N−H bending), and 1242 cm^{-1} (amide III, C−N absorption band) were marked decreased. It meant that a large number of reactive groups ($-NH_2$, −OH, and −COOH) were released due to the breaking of the peptide chain, which could be proven by the high acetaldehyde value. Since the consumption of acetaldehyde was attributed to the reactions between the acetaldehyde and amino groups of the soybean protein, a high acetaldehyde value suggested the presence of more reactions between the soybean protein liquefied product and the postadded cellulose.[35]

The inherent systems and crystalline structures of the film-forming solutions were then analyzed by using XRD measurements (Figure 2c). Two main diffraction peaks at 9.5 and 21.1° were all observed in the S1and S2, and they were attributable to the α-helices and β-sheets of the soy protein secondary structure.[39−41] Compared to the values observed for S1 and S2, the peak intensity of S2 at $2\theta \approx 9.5°$ increased, whereas that at $2\theta \approx 21.1°$ decreased, which indicated the interconversion between the secondary structures of proteins. A decreased β-sheet content led to more irregular peptide chains, attributed to the unfolding of the supramolecular spherical structure and moderate degradation of molecular chains.

3.2. Characterization and Analysis of MCC. Figure 3a shows the Fourier transform infrared spectrum of MCC from corn husks and corn husks. The characteristic peak at approximately 3331 cm^{-1} was due to the stretching vibration of the O−H groups, which could form hydrogen bonds with the other hydrophilic group. The characteristic peaks at approximately 1566, 1407, 1113, and 865 cm^{-1} disappeared in MCC, which represent the carbon skeleton vibration of the aromatic ring structure in lignin, the stretching vibration of C−O in the methoxy group, the stretching vibration of Ph−O, and the bending vibration of anomic carbon in hemicellulose, respectively. The characteristic peaks at approximately 1160, 1107, 1031, and 899 cm^{-1} belong to MCC and were attributed to the vibration of the carbon skeleton, the stretching vibration of C−O, the stretching vibration of C−O−C bonds, and the stretching vibration of the β-1,4-glycosidic bond, respec-

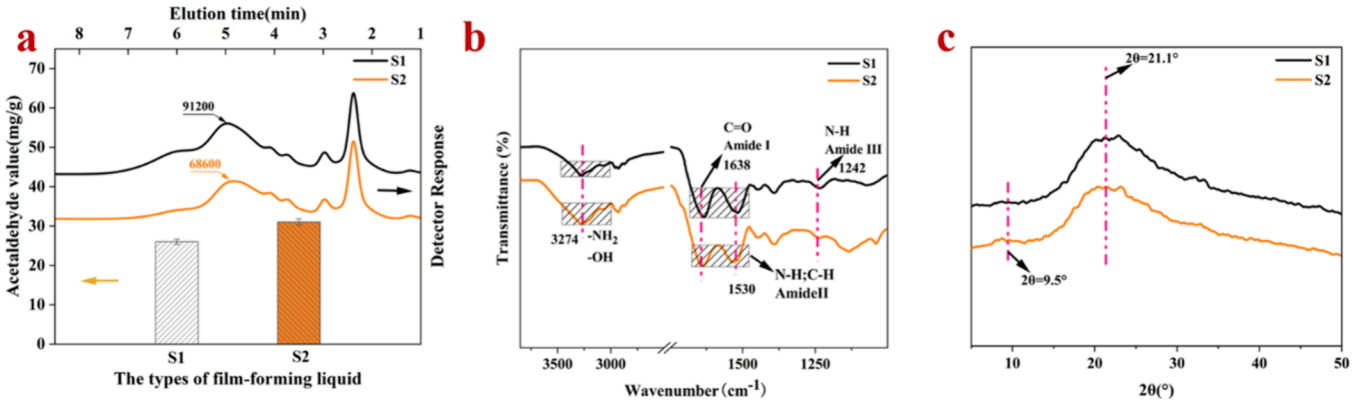

Figure 2. (a) Acetaldehyde values and GPC spectra, (b) FTIR spectra, and (c) XRD patterns of S1 and S2.

https://doi.org/10.1021/acsomega.3c07907
ACS Omega 2024, 9, 15845−15853

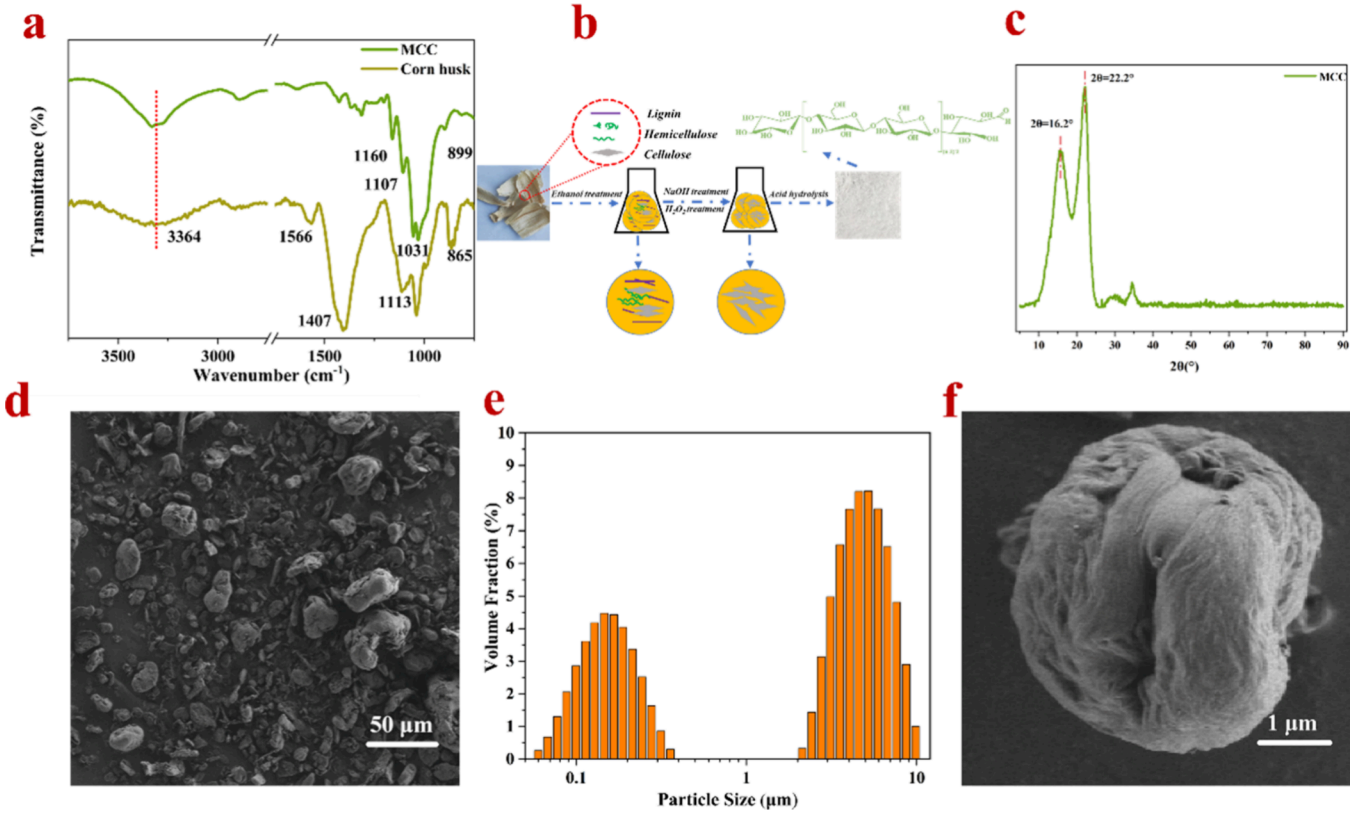

Figure 3. (a) FTIR spectra of MCC and corn husk, (b) process of preparation of MCC, (c) XRD spectrum of MCC, (e) particle size pattern of MCC, and (d,f) SEM images of MCC.

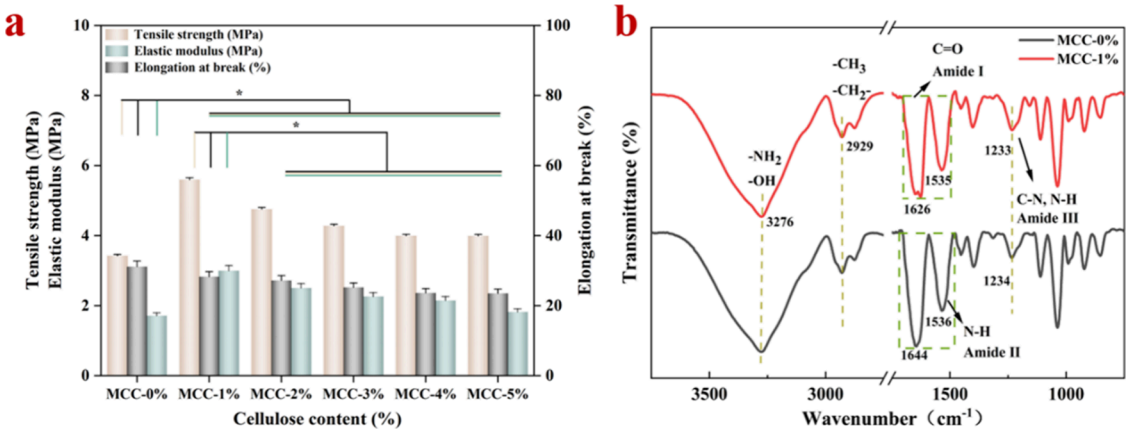

Figure 4. (a) Tensile strength, elongation at break, and elastic modulus of soy protein-based films, $*P < 0.05$. (b) FTIR spectra of "MCC-0%" and "MCC-1%".

tively.[42,43] Thus, the MCC was successfully extracted from corn husk after chemical treatment in the presence of NaOH and H_2O_2 as shown in Figure 3b. In addition, XRD analysis was conducted to evaluate the crystalline structure of MCC (Figure 3c). Characteristic diffraction peaks were observed at approximately 16.2 and 22.2°. The high crystallinity of MCC was up to 88.38% and was expected to improve the mechanical properties of the films.

SEM was used to investigate the morphology of the overview and detailed appearance of the used MCC. As shown in Figure 3d, MCC was in the state of a particulate form, and the particle dimensions were more at the micrometer level and less at the nanometer level. The same results could be obtained from the particle size test, as shown in Figure 3e. It might be inferred that the MCC exists as the aggregate of crystalline nanocellulose entities. Hundreds of individual cellulose nanofibrils form into a twine-like state, as shown in Figure 3f.

3.3. Comprehensive Analysis of Properties of Soy Protein-Based Films. The mechanical property evaluation of the soy protein-based films is shown in Figure 4a. After 1% MCC was incorporated into the soy protein-based films, the tensile strength (TS) increased significantly, from 3.4 to 5.6 MPa, the elongation at break (EB) decreased from 31.2 to 28.3%, and the elastic modulus (EM) increased from 1.7 to 3.0 MPa. However, the performance of soy protein-based films

https://doi.org/10.1021/acsomega.3c07907
ACS Omega 2024, 9, 15845−15853

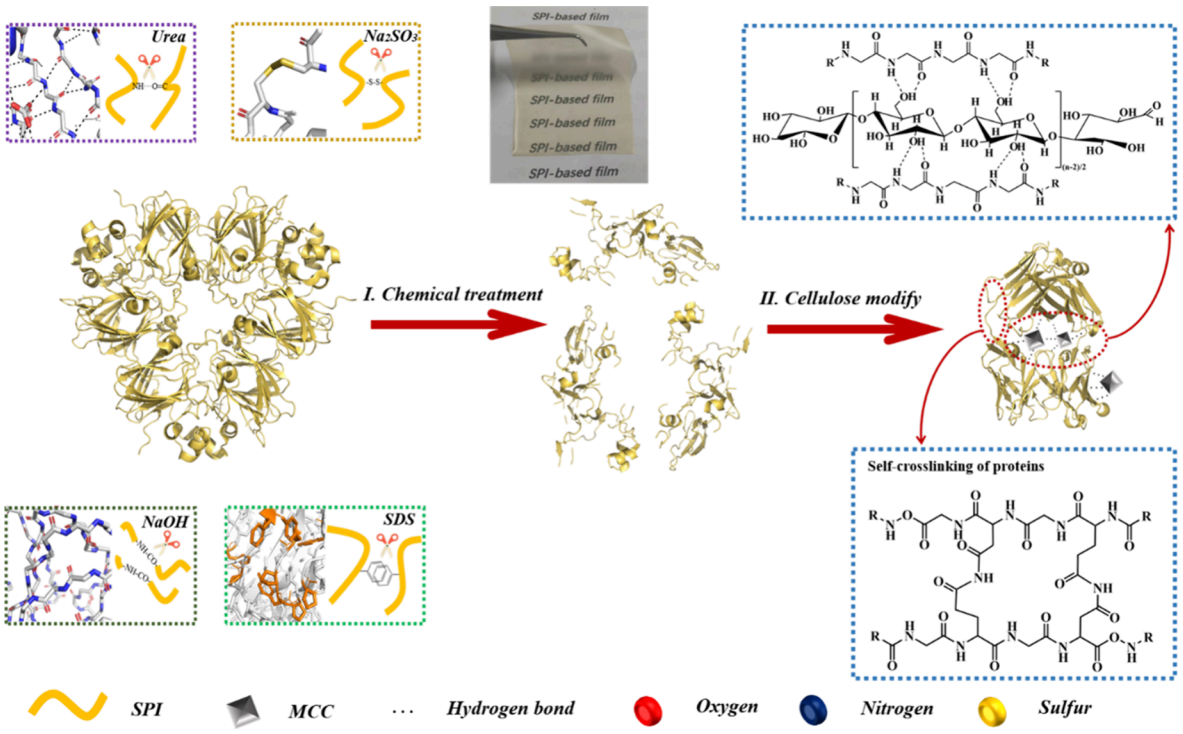

Figure 5. Schematic of the modification of the soy protein-based film.

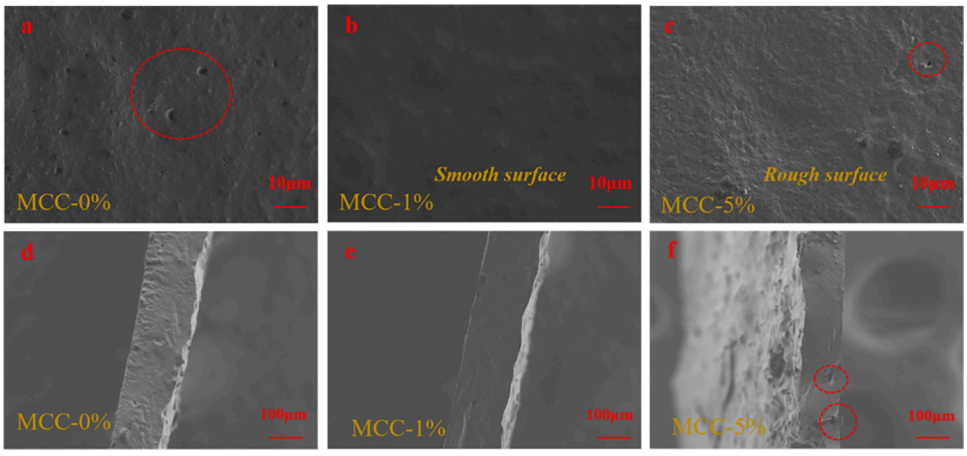

Figure 6. SEM images of surface (a–c) and fractured cross-sectional (d–f) microstructure of the "MCC-0%", "MCC-1%", and "MCC-5%".

became poor as the MCC content increased continuously. Thus, the addition of an appropriate amount of MCC could improve the performance of the soy protein-based film, which is due to moderate self-cross-linking of proteins and hydrogen bonding between proteins and MCC. The results might be explained as shown in Figure 5. Since the structure of the protein was unfolded after chemical treatment, it would release many active groups. This was followed by the process of covalent and noncovalent chemical bond remodeling between proteins or proteins and MCC, which could be proven by the FTIR analysis. It could be seen that there was no new absorption peak detected in Figure 4b, and typical infrared absorption characteristics of amide I (C═O stretching vibrations), amide II (N−H bending vibrations), and amide III (C−N stretching/N−H bending vibrations) were all detected in "MCC-0%" and "MCC-1%", indicating no apparent change in the chemical composition.[44] However, a redshift of the absorption band (amide I, from 1644 to 1626 cm^{-1}) could be detected, attributed to the formation of hydrogen bonding changing the charge distribution of the groups on the amide I. Meanwhile, the formation of hydrogen bonding could make peptide chains fold and bend slightly, thus bringing the distance between C═O closer, resulting in the infrared absorption peak of C═O stretching vibrations splitting.[45]

Figure 6 shows SEM micrographs of soy protein-based film surfaces and fractured cross sections with or without MCC. It was observed that the surface of the film produced using SPI and glycerol was uneven and had many small pores, which might be attributed to the low density. With the addition of 1% MCC, the small pores almost disappeared, and the surface became compact and smooth due to the association of the covalent (self-cross-linking of proteins) and noncovalent bonds (hydrogen bonding between protein and MCC) in the film

https://doi.org/10.1021/acsomega.3c07907
ACS Omega 2024, 9, 15845−15853

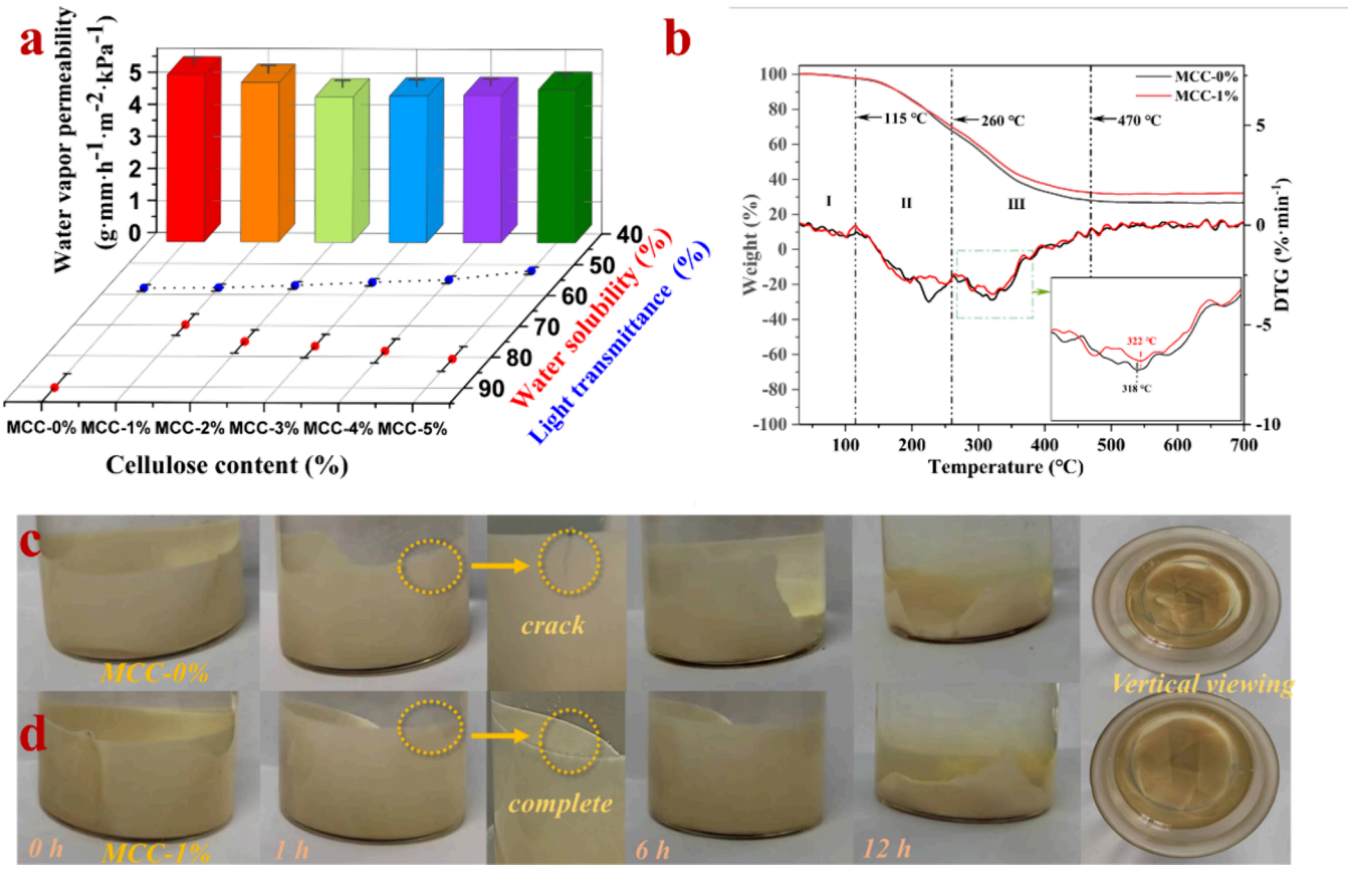

Figure 7. (a) Water vapor permeability, water solubility, and light transmittance pattern of soy protein-based films, (b) TGA and DTG curves of "MCC-0%" and "MCC-1%", and (c,d) 24 h difference images of "MCC-0%" and "MCC-1%" in water.

matrix. In addition, the fractured cross section of the film with an MCC content of 1% was also relatively smooth, indicating that the MCC was well dispersed in the SPI system, and there was good compatibility between SPI and cellulose. However, when the amount of cellulose added increased to 5%, holes appeared on the surface and fractured cross section due to the aggregation of cellulose particles.

The WVP of soy protein-based films with MCC is shown in Figure 7a, The WVP values initially decreased with the addition of the MCC content and then gradually increased but remained lower than that of the "MCC-0%" sample. Among them, "MCC-2%" exhibited the lowest WVP of 4.54 g·mm·h^{-1}·m^{-2}·kPa^{-1}. However, further increasing the MCC level to 5% obviously increased the WVP. This can be attributed to the obvious aggregation of MCC particles, resulting in the formation of new pores and the discontinuity of the polymer phase in the film, allowing water to penetrate the film layer. The results indicated that a moderate addition of MCC improved the water barrier properties of soy protein-based films. The dispersion of impermeable MCC in the SPI matrix may create a tortuous path, hindering the diffusion of water vapor.

The results of the WS demonstrated that the addition of MCC enhanced the water resistance of the soy protein-based films (Figure 7a). In Figure 7c,d, the "MCC-0%" sample exhibited cracks after soaking for 1 h and a larger area dissolution after soaking for 6 h. In addition, the "MCC-1%" had the lowest WS of 69.8% and could withstand 6 h of soaking without cracking. Meanwhile, the addition of MCC slightly decreased the light transmittance of films.

The thermal degradation process of the films of "MCC-0%" and "MCC-1%" was divided into three stages, where stage I ranged from 30 to 115 °C, stage II ranged from 115 to 260 °C, and stage III ranged from 260 to 470 °C. The degradation of stage I was attributed to the generation of vapor and gases by the curing reaction of the soy protein-based films. At the range from 115 to 470 °C, severe weight losses occurred in all samples, which are associated with the decomposition of the film's skeleton structure, where stage II was attributed to the destruction of the unstable chemical structures of the soy protein-based films and stage III was attributed to the degradation of peptide bonds in the soy protein backbone. The maximal degradation temperature of the "MCC-0%" was 318 °C. As shown in Figure 7b, after the addition of MCC into the soy protein-based films, the maximal degradation temperature was increased to 322 °C. The improvement of the thermal stability was ascribed to the construction of a stable structure. In addition, the thermal degradation rate at the degradation temperature of the range from 260 to 470 °C was significantly reduced. These results indicated that the chemical treatment combined with biomass enhancement endowed the "MCC-1%" with better thermal degradation resistance and improved thermo-stability.

4. CONCLUSIONS

In summary, the modification of soybean protein, in combination with chemical reagents such as sodium sulfite, sodium dodecyl sulfate, urea, and sodium hydroxide, along with the reinforcement of MCC, has a significant impact on the properties of soy protein-based films. SPI was dispersed in

https://doi.org/10.1021/acsomega.3c07907
ACS Omega 2024, 9, 15845−15853

the film-forming solution after its supramolecular spherical structure was unfolded and underwent moderate degradation of molecular chains. Subsequently, self-cross-linking occurred between the proteins and with MCC took place through hydrogen bonds. In addition, MCC, which possesses a significant surface area along with high toughness and strength, could form evenly distributed fine fibers after being incorporated into soy protein-based films. This synergistic combination resulted in soy protein-based films with excellent mechanical strength, low water solubility, and low water vapor permeability. Therefore, the proposed film of "MCC-1%" could withstand 6 h of soaking without cracking and has high TS and EM and lower EB strength of 5.6 MPa, 3.0 MPa, and 28.3%, respectively. It is crucial to broaden the application of soy protein-based films proposed by chemical treatment combined with biomass enhancement. The improvements in these performance aspects enhance the packaging application scope of soy protein-based films, providing assurance for food storage and transportation. Considering that the addition of MCC may decrease the EB of soy protein-based films, future efforts can focus on modifying MCC or incorporating suitable toughening agents to enhance the toughness of soy protein-based films.

AUTHOR INFORMATION

Corresponding Authors

Binghan Zhang − *College of Chemistry and Chemical Engineering, Heze University, Heze, Shandong 274015, China*; orcid.org/0000-0002-6825-802X; Email: 18346186030@163.com

Jinguo Wang − *Heze Forestry Administration, Heze, Shandong 274015, China*; Email: wjg001001@163.com

Authors

Baicheng Guo − *College of Chemistry and Chemical Engineering, Heze University, Heze, Shandong 274015, China*

Shihan Wang − *College of Chemistry and Chemical Engineering, Heze University, Heze, Shandong 274015, China*

Can Liu − *Yunnan Provincial Key Laboratory of Wood Adhesives and Glued Products, Southwest Forestry University, Kunming, Yunnan 650224, China*

Lu Cheng − *College of Chemistry and Chemical Engineering, Heze University, Heze, Shandong 274015, China*

Complete contact information is available at: https://pubs.acs.org/10.1021/acsomega.3c07907

Notes

The authors declare no competing financial interest.

ACKNOWLEDGMENTS

This study (no. 2022-JNJ02) was funded by the Yunnan Provincial Key Laboratory of Wood Adhesives and Glued Products (Southwest Forestry University) and supported by the 111 Project (D21027).

REFERENCES

(1) González, A.; Gastelu, G.; Barrera, G.; Ribotta, P. D.; Igarzabal, C. I. A. *Preparation and characterization of soy protein films reinforced with cellulose nanofibers obtained from soybean by-products*. Elsevier 2019.

(2) Cazón, P.; Velazquez, G.; Ramírez, J. A.; Vázquez, M. Polysaccharide-based films and coatings for food packaging: A review. *Food Hydrocolloids* **2016**, *68*, 136−148.

(3) Thakur, R.; Pristijono, P.; Scarlett, C. J.; Bowyer, M.; Singh, S. P.; Vuong, Q. V. Starch-based films: Major factors affecting their properties. *Int. J. Biol. Macromol.* **2019**, *132*, 1079 DOI: 10.1016/j.ijbiomac.2019.03.190.

(4) Las Heras, K.; Santos-Vizcaino, E.; Garrido, T.; Gutierrez, F. B.; Aguirre, J. J.; de la Caba, K.; Guerrero, P.; Igartua, M.; Hernandez, R. M. Soy protein and chitin sponge-like scaffolds: from natural by-products to cell delivery systems for biomedical applications. *Green Chem.* **2020**, *22*, 3445 DOI: 10.1039/D0GC00089B.

(5) Bortolatto, R.; Bittencourt, P. R. S.; Yamashita, F. Biodegradable starch/polyvinyl alcohol composites produced by thermoplastic injection containing cellulose extracted from soybean hulls (Glycine max L.). *Ind. Crops Prod.* **2022**, *176*, No. 114383.

(6) Li, X.; Wei, Y.; Jiang, S.; Zhou, Y.; Li, J.; Li, K.; Shi, S. Q.; Li, J. Full Bio-Based Soy Protein Isolate Film Enhanced by Chicken Feather Keratin. *Macromol. Mater. Eng.* **2021**, 2100004.

(7) Jensen, A.; Lim, L. T.; Barbut, S.; Marcone, M. Development and characterization of soy protein films incorporated with cellulose fibers using a hot surface casting technique. *LWT - Food Science and Technology* **2015**, *60* (1), 162−170.

(8) Sugawara, K.; Fukushi, H.; Hoshi, S.; Akatsuka, K. Electrochemical sensing of glucose at a platinum electrode with a chitin/glucose oxidase film. *Analytical sciences* **2000**, *16* (11), 1139−1143.

(9) Cunha, C. S.; Castro, P. J.; Sousa, S. C.; Pullar, R. C.; Tobaldi, D. M.; Piccirillo, C.; Pintado, M. M. Films of chitosan and natural modified hydroxyapatite as effective UV-protecting, biocompatible and antibacterial wound dressings. *International Journal of Biological Macromolecules* **2020**, *159*, 1177−1185.

(10) Chao, Z.; Yue, M.; Xiaoyan, Z.; Dan, M. Development of Soybean Protein-Isolate Edible Films Incorporated with Beeswax, Span 20, and Glycerol. *J. Food Sci.* **2010**, *75* (6), C493−C497.

(11) Mir, N. A.; Riar, C. S.; Singh, S. Structural modification in album (Chenopodium album) protein isolates due to controlled thermal modification and its relationship with protein digestibility and functionality. *Food Hydrocolloids* **2020**, *103*, No. 105708.

(12) Wihodo, M.; Moraru, C. I. Physical and chemical methods used to enhance the structure and mechanical properties of protein films: A review. *Journal of food engineering* **2013**, *114* (3), 292−302.

(13) Xu, Y.; Han, Y.; Chen, M.; Li, J.; Li, J.; Luo, J.; Gao, Q. A soy protein-based film by mixed covalent and flexibilizing networks. *Industrial Crops and Products* **2022**, *183*, No. 114952.

(14) Jiang, Y.; Tang, C.; Wen, Q.; Li, L.; Yang, X. Effect of processing parameters on the properties of transglutaminase-treated soy protein isolate films. *Innovative Food Science & Emerging Technologies* **2007**, *8* (2), 218−225.

(15) Park, S. K.; Rhee, C. O.; Bae, D. H.; Hettiarachchy, N. S. Mechanical Properties and Water-Vapor Permeability of Soy-Protein Films Affected by Calcium Salts and Glucono-*δ*-lactone. *J. Agric. Food Chem.* **2001**, 2308 DOI: 10.1021/jf0007479.

(16) Zhou, J. J.; Wang, S. Y.; Gunasekaran, S. Preparation and Characterization of Whey Protein Film Incorporated with TiO2 Nanoparticles. *J. Food Sci.* **2009**, *74* (7), N50−N56.

(17) Wang, Z.; Zhou, J.; Wang, X. X.; Zhang, N.; Sun, X. X.; Ma, Z. S. The effects of ultrasonic/microwave assisted treatment on the water vapor barrier properties of soybean protein isolate-based oleic acid/stearic acid blend edible films. *Food Hydrocolloids* **2014**, *35*, 51−58.

(18) Jiang, J.; Xiong, Y. L.; Newman, M. C.; Rentfrow, G. K. Structure-modifying alkaline and acidic pH-shifting processes promote film formation of soy proteins. *Food Chem.* **2012**, *132* (4), 1944−1950.

(19) Wang, D.; Qi, B.; Xu, Q.; Zhang, S.; Xie, F.; Li, Y. Effect of salt ions on an ultrasonically modified soybean lipophilic protein nanoemulsion. *International Journal of Food Science & Technology* **2021**, *56* (12), 6719−6731.

(20) Huang, W.; Sun, X. Adhesive properties of soy proteins modified by urea and guanidine hydrochloride. *J. Am. Oil Chem. Soc.* **2000**, *77* (1), 101−104.
(21) Schmidt, V.; Giacomelli, C.; Soldi, V. Thermal stability of films formed by soy protein isolate−sodium dodecyl sulfate. *Polymer degradation and stability* **2005**, *87* (1), 25−31.
(22) Liu, P.; Xu, H.; Zhao, Y.; Yang, Y. Rheological properties of soy protein isolate solution for fibers and films. *Food Hydrocolloids* **2017**, *64*, 149−156.
(23) Qin, Z.; Mo, L.; Liao, M.; He, H.; Sun, J. Preparation and characterization of soy protein isolate-based nanocomposite films with cellulose nanofibers and nano-silica via silane grafting. *Polymers* **2019**, *11* (11), 1835.
(24) Xie, W.-Y.; Wang, F.; Xu, C.; Song, F.; Wang, X.-L.; Wang, Y.-Z. A superhydrophobic and self-cleaning photoluminescent protein film with high weatherability. *Chemical Engineering Journal* **2017**, *326*, 436−442.
(25) Dai, L.; Wang, X.; Jiang, X.; Han, Q.; Jiang, F.; Zhu, X.; Xiong, C.; Ni, Y. Role of nanocellulose in colored paper preparation. *International Journal of Biological Macromolecules* **2022**, *206*, 355−362.
(26) Sukyai, P.; Anongjanya, P.; Bunyahwuthakul, N.; Kongsin, K.; Harnkarnsujarit, N.; Sukatta, U.; Sothornvit, R.; Chollakup, R. Effect of cellulose nanocrystals from sugarcane bagasse on whey protein isolate-based films. *Food Research International* **2018**, *107*, 528−535.
(27) Huang, S.; Tao, R.; Ismail, A.; Wang, Y. Cellulose nanocrystals derived from textile waste through acid hydrolysis and oxidation as reinforcing agent of soy protein film. *Polymers* **2020**, *12* (4), 958.
(28) Yang, X.; Han, F.; Xu, C.; Jiang, S.; Huang, L.; Li, L.; Xia, Z. Effects of preparation methods on the morphology and properties of nanocellulose (NC) extracted from corn husk. *Ind. Crops Prod.* **2017**, *109*, 241−247.
(29) Ratna, A. S.; Ghosh, A.; Mukhopadhyay, S. Advances and prospects of corn husk as a sustainable material in composites and other technical applications. *Journal of cleaner production* **2022**, *371*, No. 133563.
(30) Jiang, K.; Zhang, J.; Xia, S.; Ou, C.; Fu, C.; Yi, M.; Li, W.; Jing, M.; Lv, W.; Xiao, H. Improve performance of soy protein adhesives with a low molar ratio melamine-urea-formaldehyde resin. *J. Phys.: Conf. Ser.* 2020, IOP Publishing *1549*, 032083
(31) Zhong, Z.; Sun, X. S.; Fang, X.; Ratto, J. A. Adhesion strength of sodium dodecyl sulfate-modified soy protein to fiberboard. *Journal of adhesion science and technology* **2001**, *15* (12), 1417−1427.
(32) Zhang, B.; Wang, J.; Zhang, F.; Wu, L.; Guo, B.; Gao, Z.; Zhang, L. Preparation of a high-temperature soybean meal-based adhesive with desired properties via recombination of protein molecules. *ACS omega* **2022**, *7* (27), 23138−23146.
(33) Liu, J.; Wang, L.; Li, J.; Li, C.; Zhang, S.; Gao, Q.; Zhang, W.; Li, J. Degradation mechanism of Acacia mangium tannin in NaOH/urea aqueous solution and application of degradation products in phenolic adhesives. *International Journal of Adhesion and Adhesives* **2020**, *98*, No. 102556.
(34) Li, J.; Zhang, B.; Li, X.; Yi, Y.; Shi, F.; Guo, J.; Gao, Z. Effects of typical soybean meal type on the properties of soybean-based adhesive. *International Journal of Adhesion and Adhesives* **2019**, *90*, 15−21.
(35) Zhang, B.; Li, J.; Kan, Y.; Gao, J.; Zhang, Y.; Gao, Z. The Effect of Thermo-Chemical Treatment on the Water Resistance of Defatted Soybean Flour-Based Wood Adhesive. *Polymers* **2018**, *10* (9), 955 DOI: 10.3390/polym10090955.
(36) Bertuzzi, M. A.; Vidaurre, E. F. C.; Armada, M.; Gottifredi, J. C. Water vapor permeability of edible starch based films. *J. Food Eng.* **2007**, *80* (3), 972−978.
(37) Gao, Z.-H.; Zhang, Y.-H.; Fan, B.; Zhang, L.-P.; Shi, J. The Effects of Thermal-Acid Treatment and Crosslinking on The Water Resistance of Soybean Protein. *Ind. Crops Prod.* **2015**, *74*, 122−131.
(38) Kumar, R.; Choudhary, V.; Mishra, S.; Varma, I. K.; Mattiason, B. Adhesives and plastics based on soy protein products. *Industrial crops and products* **2002**, *16* (3), 155−172.
(39) Liu, X.; Wang, K.; Gu, W.; Li, F.; Li, J.; Zhang, S. Reinforcement of interfacial and bonding strength of soybean meal-based adhesive via kenaf fiber−CaCO3 anchored N-cyclohexyl-2-benzothiazole sulfenamide. *Composites Part B: Engineering* **2018**, *155*, 204−211.
(40) Zhang, Y.; Liu, Z.; Xu, Y.; Li, J.; Shi, S.; Li, J.; Gao, Q. High performance and multifunctional protein-based adhesive produced via phenol-amine chemistry and mineral reinforcement strategy inspired by arthropod cuticles. *Chemical Engineering Journal* **2021**, *426*, No. 130852.
(41) Chen, S.; Fan, D.; Gui, C. Investigation of humidity-heat aging resistance of a soy protein adhesive fabricated by soybean meal and lignin-based polymer. *Polymer Testing* **2023**, *120*, No. 107971.
(42) Lei, W.; Fang, C.; Zhou, X.; Yin, Q.; Pan, S.; Yang, R.; Liu, D.; Ouyang, Y. Cellulose nanocrystals obtained from office waste paper and their potential application in PET packing materials. *Carbohydr. Polym.* **2018**, *181*, 376−385.
(43) Hemmati, F.; Jafari, S. M.; Kashaninejad, M.; Motlagh, M. B. Synthesis and characterization of cellulose nanocrystals derived from walnut shell agricultural residues. *Int. J. Biol. Macromol.* **2018**, *120*, 1216−1224.
(44) Han, Y.; Yu, M.; Wang, L. Preparation and characterization of antioxidant soy protein isolate films incorporating licorice residue extract. *Food Hydrocolloid* **2018**, *75*, 13−21.
(45) Steiner, T. The hydrogen bond in the solid state. *Angewandte Chemie International Edition* **2002**, *41* (1), 48−76.

https://doi.org/10.1021/acsomega.3c07907
ACS Omega 2024, 9, 15845−15853